Optik - International Journal for Light and Electron Optics 203 (2020) 163973

Contents lists available at ScienceDirect

Optik

journal homepage: www.elsevier.com/locate/ijleo

Enhanced subwavelength photonic nanojet focusing via a graded-index round-head microcylinder

Haidong Zhang[a,b,*]

[a] Changchun Institute of Optics, Fine Mechanics and Physics, Chinese Academy of Science, Changchun, 130033, China
[b] Center of Materials Science and Optoelectronics Engineering, University of Chinese Academy of Sciences, Beijing, 100049, China

ARTICLE INFO

Keywords:
Photonic nanojet
Graded-index
Microcylinder

ABSTRACT

Photonic nanojet is a sub-wavelength focus generated by a dielectric microparticle, like microsphere and microcylinder. The formation of nanojet can be tuned by changing the refractive index distribution and geometrical parameters of the structure. Many applications based on photonic nanojet have been explored based on the special property of dielectric microparticles. In this letter, a graded-index structure that combines hemisphere and microcylinder is proposed, which can generate a sub-wavelength nanojet with a full width at a half maximum of 120.9 nm (0.24 λ with 500 nm illumination wavelength). The influences of refraction index distribution and the length of cylinder on the properties of photonic nanojet are simulated and discussed. Moreover, the sensitivity of fabrication errors is analyzed to verify the feasibility of this structure.

1. Introduction

Photonic nanojet (PNJ) is a sub-wavelength high-intensity focus, which can be obtained at the shadow side of dielectric microparticles, like the microsphere and microcylinder with plane wave illumination. The scattering mechanism can be well described by Mie theory, which rigorously solves Maxwell's equations with a quasi-analytical solution. It has attracted great attentions since the PNJ was firstly introduced by Chen et al. via finite-difference-time-domain (FDTD) simulation of a cylinder illuminated by a plane wave [1]. A variety of applications based on PNJ have been proposed since the full width at half maximum (FWHM) at focal plane is ultra-narrow. It was experimentally demonstrated that holes of diameter less than 100 nm can be fabricated in various materials under the microsphere, and arbitrary structure patterns can be done through off-axis irradiation of microsphere [2]. Furthermore, the resolution of an optical microscope can be improved down to tens of nanometers with a microsphere integrated to the traditional microscope [3–6]. Many other promising applications have been reported including optical storage, smart sensing and Raman spectroscopy [7–9].

The study on the PNJ focusing was also widely reported in recent years and it has been demonstrated that the size and optical properties of PNJ are strongly dependent on the geometrical shape and optical parameters of the microparticle illuminated [10–13]. The refractive index distribution of the structure has a significant impact on the formation of PNJ, like elongated or super narrow PNJ [14–16]. A PNJ with a length of around 20 wavelengths can be generated by the graded-index microsphere at the cost of larger FWHM and weaker peak intensity [17]. Similarly, the phenomenon can be found in graded-index micro-cuboid [18]. In addition, as the most significant property of PNJ, enhanced subwavelength focusing has been wildly studied. A PNJ with a reduced FWHM of 0.3 λ can be achieved by using the pupil masks on the center of microsphere [19]. However, the peak intensity of PNJ is quite low since a

* Corresponding author at: Changchun Institute of Optics, Fine Mechanics and Physics, Chinese Academy of Science, Changchun, 130033, China.
E-mail address: zhanghaidong15@mails.ucas.edu.cn.

https://doi.org/10.1016/j.ijleo.2019.163973
Received 15 October 2019; Accepted 3 December 2019

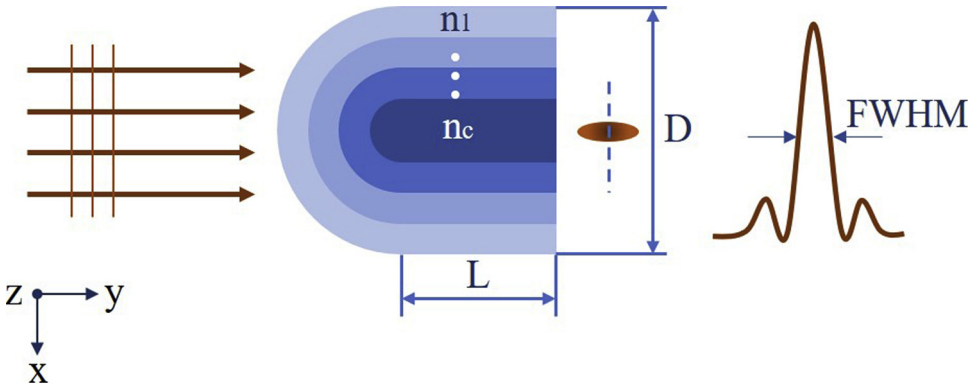

Fig. 1. Schematic of the model of graded-index round-head microcylinder.

certain amount of energy is blocked by the mask.

In this study, a graded-index round-head microcylinder structure is proposed, which is made up of a cylinder and a hemisphere. The enhanced sub-wavelength PNJ with a FWHM of 120.9 nm (0.24 λ with 500 nm incident light wavelength) can be obtained by numerical simulation. This is important for advanced microsphere-based technology, like nanofabrication and imaging. The influences of refractive index distribution and length of cylinder are discussed. The sensitivity of fabrication errors is also analyzed.

2. Proposed microstructure

The geometric parameters and refractive index model of the graded-index round-head cylinder, and characteristics of PNJ are illustrated in Fig. 1. The microparticle is made up of a hemisphere and a cylinder. The diameter of hemisphere and cylinder is denoted as D, and the length of cylinder is denoted as L. This 3D round-head microcylinder with several (N) layers is the core-shell structure. The thickness of each layer is the same and the refractive index is homogeneous. To describe the distribution of refractive index, refractive index grading type 'g' is defined by the equation

$$\frac{n_m}{n_c} = \left(\frac{n_1}{n_c}\right)^{\left(\frac{N-m}{N-1}\right)^g}, \tag{1}$$

where m means the mth layer with refractive index n_m. n_c and n_1 are the refractive indices of the innermost and outermost layer, respectively. The range of refractive index of each shell is partly limited by the modern coating technology. The materials with refractive index range of 1.05–2.0 have been reported with different compositions and porosities of silica glass [20].

The microcylinder is illuminated by a linear polarized plane wave at a wavelength of 500 nm. The direction of propagation is along y axis, while the polarization direction is parallel to x axis.

To investigate the performance of PNJ, the finite-difference time-domain (FDTD) method is employed in the numerical simulation. To ensure the high accuracy of simulation, the spatial lattice of FDTD is set to 10 nm. The key parameters of PNJ are peak intensity and FWHM at the focal plane. One key point should be noted that the FWHM is measured at the peak intensity plane outside the structure, instead of the peak intensity plane of the focus, if the peak intensity of focus is inside the structure.

3. Simulation results and discussion

In this study, the diameter D of the hemisphere and cylinder is 4 μm with 3 layers of thickness d = 500 nm coated on the surface of the core successively. The typical refractive index of innermost and outermost layer is set to 1.9 and 1.4, respectively. The refractive index grading type 'g' = 1 and the refractive index of the rest layers are defined by Eq. (1). The length of cylinder L = 0.9 μm. To verify the advantages of round-head graded-index microcylinder, homogeneous microspheres of same diameter with refractive indices of 1.4 & 1.9, and graded-index microsphere with refractive index ranges from 1.9 to 1.4 in g = 1 are also simulated with the plane wave illumination at 500 nm.

In Fig. 2(a) and (b), electric intensity of microspheres with homogeneous refractive index of 1.4 & 1.9 are shown, respectively. Fig. 2(c) & (d) are electric intensity of graded-index microsphere and round-head cylinder with refractive index range from 1.4 to 1.9, and the gradient type 'g' is equal to 1. Fig. 2(e) & (f) are the transverse and axial intensity profiles of PNJ generated by the structures above. It can be figured out that a typical photonic nanojet is generated by the microsphere at a refractive index of 1.4, and the whole nanojet is outside the microsphere. The FWHM of this PNJ is 268.47 nm (0.537 λ), which has been plotted in Fig. 2(e). As the refractive index increases, the microsphere has more ability to refract and converge the light. The PHJ gets narrower, and it moves into the microsphere gradually. While the refractive index increases to 1.9, the PNJ focuses almost entirely inside the microsphere. The light intensity on the external surface of microsphere is quite weak, as shown in Fig. 2(e), and the corresponding FWHM is 291.8 nm (0.584 λ). Similar phenomenon occurs on the graded-index microsphere. The PNJ is fully inside the microsphere, which can be seen clearly in the axial intensity profile of PNJs (Fig. 2(f)). Since the intensity at the external surface of this graded-index

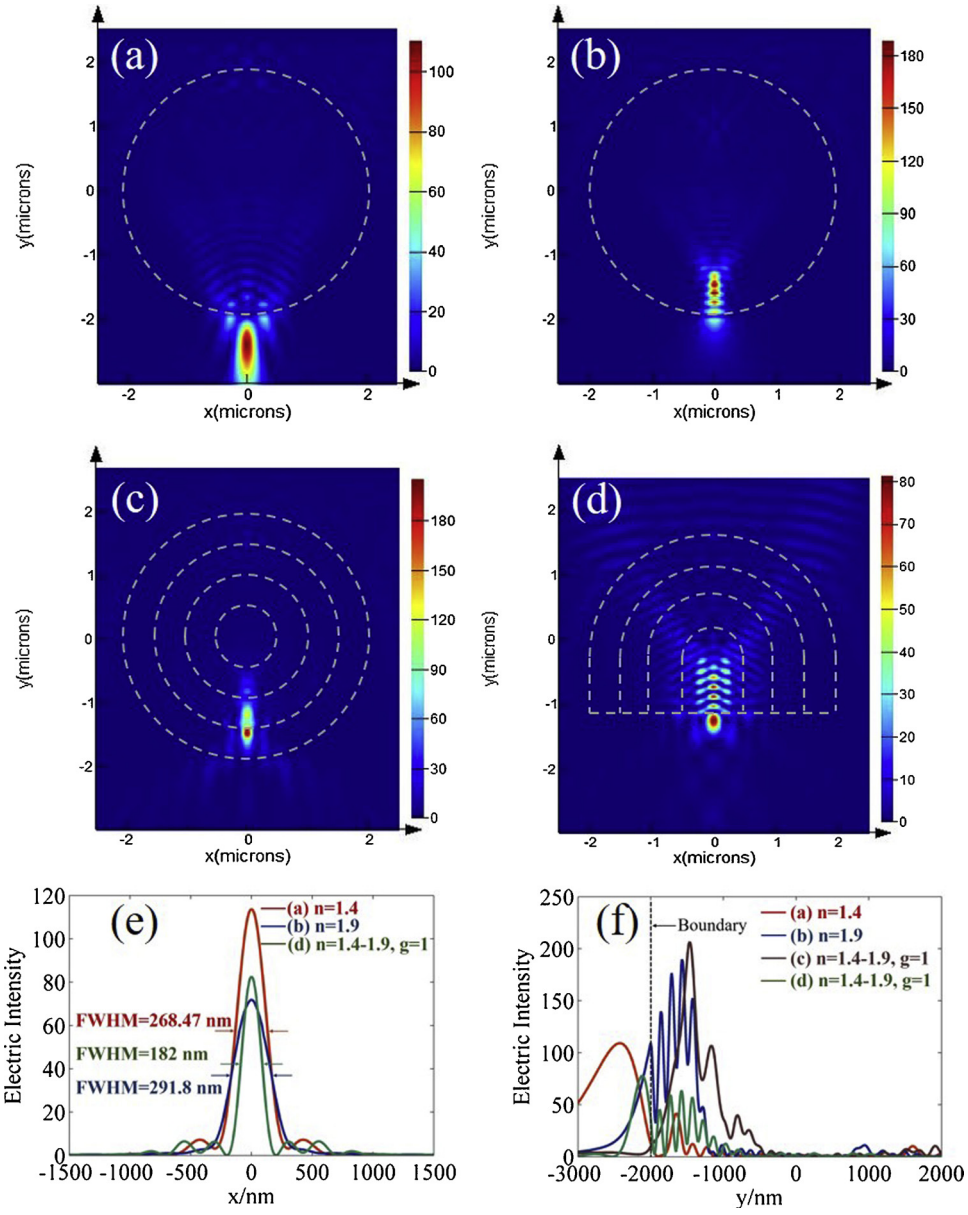

Fig. 2. (a) & (b) Electric intensities of microsphere with homogeneous refractive index of 1.4 & 1.9, respectively. (c) & (d) Electric intensities of graded-index microsphere and round-head microcylinder with refractive index range from 1.4 to 1.9, and g = 1. (e) & (f) Transverse and axial intensity profiles of PNJ generated by the structures above.

microsphere is ignorable, compared to other simulation results, the corresponding transverse intensity profile is not shown in Fig. 2(e). From the simulation result of round-head graded-index cylinder shown in Fig. 2(d), it is clear that the peak intensity is outside the microcylinder, and the FWHM obtained by this structure is 182 nm (0.364 λ), which is the smallest one among these four comparative simulations. There exist several peak intensities inside the round-head cylinder, it is a superposition of waves from different shells and radial distances. When a plane wave incidents to the hemisphere, the incident angle differs along the radial direction. It results in different turning angles when the light arrives into the core part of the structure through several shells.

When light passes through a medium, the direction of propagation deflects to the region where the refractive index is higher than surroundings. For the graded-index microsphere, the refractive index of core is higher than the outer shells along all directions, thus, the energy is focused close to the center of microsphere. This explains the phenomenon that the PNJ generated by the graded-index microsphere is fully inside the structure compared to the microsphere with refractive index of 1.9. While for the graded-index round-head cylinder, the plane wave is firstly converged by the hemisphere. In the cylindrical structure, the refractive index only changes in the x-z plane, and the refractive along y axis remains the same. In this condition, the energy can be transmitted further along the y axis.

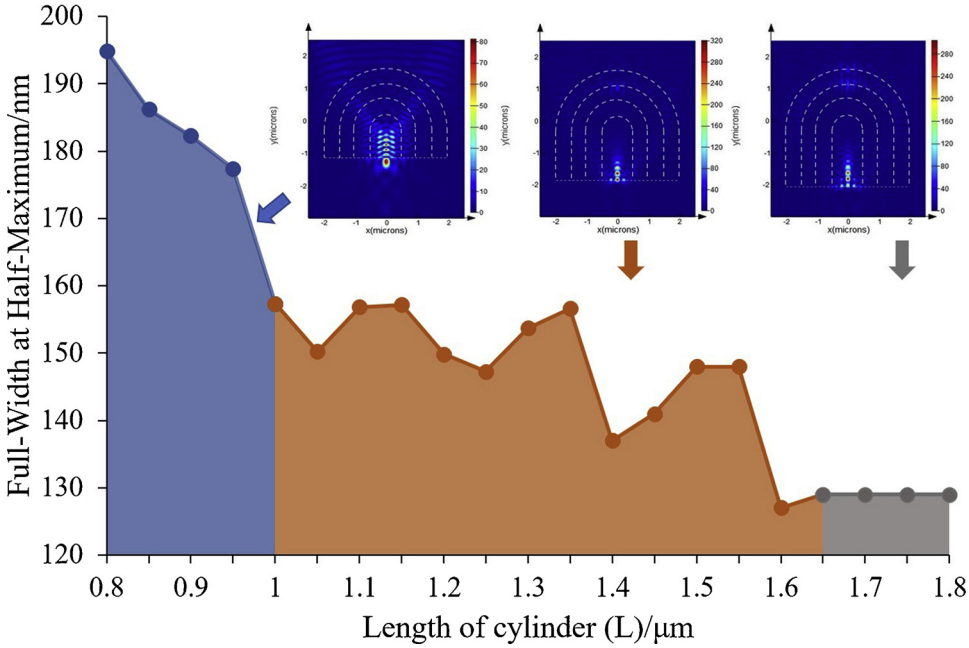

Fig. 3. The FWHM of PNJ versus the length of cylinder. Three typical electric intensity distributions for different conditions are shown in the inserts.

The length of microcylinder 'L' also has a significant effect on the properties of PNJ. Short length results in a PNJ of large FWHM, while long length can achieve a narrower PNJ with more risks to be focused inside the structure. Several simulations of different lengths are conducted to verify the assumption under the same condition as Fig. 2(d).

The length of cylinder ranges from 0.8 to 1.8 μm, and the variation trend of FWHM of PNJ is depicted in Fig. 3. From the simulation, it can be divided into three conditions. The typical electric field intensity distributions of three conditions are shown in the inserts, and the cylinder heights are 0.9, 1.6, and 1.8 μm correspondingly. When the height is less than 1.0 μm, the PNJ is focused outside the round-head microcylinder, and the FWHM decreases as the height increases. When the height is beyond 1.65 μm, the PNJ is fully focused inside the structure, which is not what we are interested in, since this condition cannot make much sense in practice. When the height ranges from 1.0 to 1.65 μm, the PNJ is partly outside the structure. It is shown that the FWHM of external surface of cylinder cyclically decreases with the increase of the height. The narrowest PNJ with the FWHM of 120.9 nm (0.24 λ) can be obtained when the height of cylinder is 1.6 μm. Also, the peak intensity of this PNJ is 219, while the intensity of microsphere with homogeneous index 1.4 is 114. It can be explained that with the increase of length, there exist some specific heights of cylinder that make interference enhanced on the external surface of cylinder, like L = 1.05 μm, 1.25 μm, 1.4 μm, and 1.6 μm.

The refractive index distribution also makes a big difference on the PNJ, which has been reported in other graded-index structures [10,14,16]. For the round-head microcylinder, we first consider the effect of n_1 on the formation of PNJ. The refractive index of outermost layer n_1 changes from 1.7 to 1.9, and other parameters keep the same. As is shown in Fig. 4, when n_1 is equal to 1.75, the FWHM of PNJ is 161 nm (0.322 λ), and the side lobes are quite small compared to the main lobe. With the increase of n_1, the energy is transformed gradually from central lobe to side lobes, and the FWHM decreases correspondingly. When n_1 is equal to 1.9, the FWHM

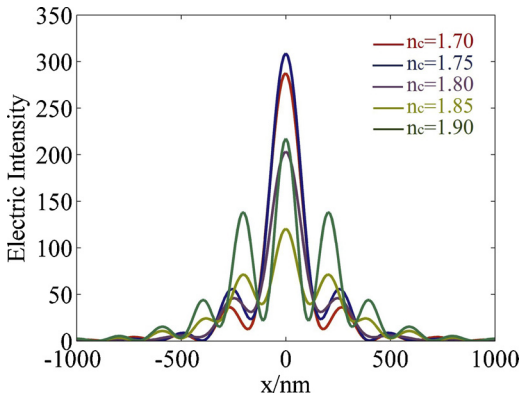

Fig. 4. Transverse intensity profiles of PNJs generated by graded-index round-head microcylinders with different refractive index of core 'n_c'.

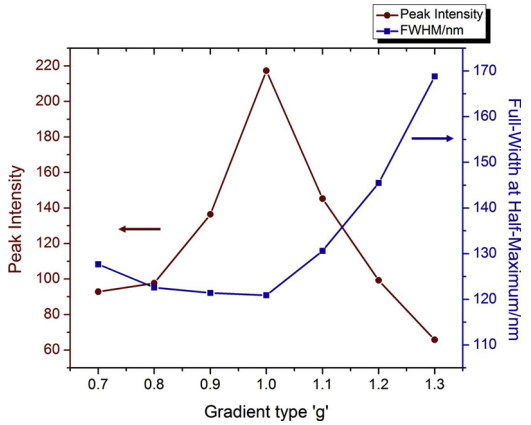

Fig. 5. Peak intensity and FWHM of PNJs generated by graded-index round-head cylinders for different gradient types 'g'.

of the external surface of microcylinder is 120.9 nm (0.24 λ).

In a similar way, we study the influence of the parameter 'g'. As shown in Fig. 5, when $g < 1.0$, the peak intensity gets higher and the FWHM decreases, while the peak intensity gets lower and the FWHM increases when $g > 1.0$. The optimal property of PNJ can be achieved when $g = 1.0$.

4. Sensitivity analysis of fabrication errors

This structure can be fabricated by ion implantation and coating technologies like atomic layer deposition, which has strong ability to coat films on the surface of 3D structure with uniform thickness. To verify the feasibility of this graded-index round-head cylinder structure, the influences of film thickness and refractive index deviation on the formation of PNJ are analyzed. We here take the innermost and outermost layer as examples to analyze the fabrication sensitivity. The thickness of layers is changed by 5 nm, 25 nm and 50 nm, respectively, and refractive index is changed by 0.01, 0.001 and 0.0001, respectively. The FWHM variation due to the fabrication errors is shown in Table 1.

From the fabrication sensitivity, we can discover that the thickness of outermost layer has more influence on the FWHM of PNJ than the innermost layer, while the refraction index of innermost layer has more influence on the FWHM of PNJ than the outermost layer. When the refraction index of innermost layer changes by 0.01, the FWHM of PNJ changes by 3 nm. When the thickness of outermost layer changes by 50 nm, the FWHM of PNJ changes by 3.8 nm, which is acceptable in fabrication.

5. Conclusion

In summary, we propose a new structure, graded-index round-head microcylinder, to generate enhanced sub-wavelength PNJ. This structure has unique advantages compared to homogeneous and graded-index microsphere. The key parameters of PNJ formed by this structure with different geometric shapes and refractive index distributions are discussed. A PNJ with the FWHM of 120.9 nm (0.24 λ with 500 nm illumination wavelength) can be obtained in the condition of $n_c = 1.9$, $n_1 = 1.4$, $g = 1$, and $L = 1.6$ μm. The

Table 1
Errors sensitivity analyses for refractive index and film thickness.

n	g	Height of cylinder/μm	Thickness of the layer/nm	FWHM/nm
innermost layer				
1.4-1.89	1	1.6	500	**123**
1.4-1.899	1	1.6	500	**120.32**
1.4-1.8999	1	1.6	500	**120**
1.4-1.9	1	1.6	*500*	**120**
1.4-1.9	1	1.6	*505*	**120.08**
1.4-1.9	1	1.6	*525*	**120.59**
1.4-1.9	1	1.6	*550*	**121.52**
outermost layer				
1.39-1.9	1	1.6	500	**121.22**
1.399-1.9	1	1.6	500	**120.04**
1.3999-1.9	1	1.6	500	**120.03**
1.4-1.9	1	1.6	*500*	**120**
1.4-1.9	1	1.6	*505*	**120.16**
1.4-1.9	1	1.6	*525*	**121.38**
1.4-1.9	1	1.6	*550*	**123.88**

peak intensity is up to 2 times that of microsphere with homogeneous index of 1.4. The formation of PNJ can be tuned via changing the length of cylinder and the refractive index distribution. The sensitivity of fabrication errors is analyzed that the tolerance of errors for this structure fabrication is acceptable for modern coating technology.

Acknowledgements

This research was funded by National Key Research and Development program (2016YFB0500100); and China Scholarship Council (201804910813)

References

[1] Z.G. Chen, A. Taflove, V. Backman, Photonic nanojet enhancement of backscattering of light by nanoparticles: a potential novel visible-light ultramicroscopy technique, Opt. Express 12 (2004) 1214, https://doi.org/10.1364/opex.12.001214.
[2] L. Chen, Y. Zhou, Y. Li, M. Hong, Microsphere enhanced optical imaging and patterning: from physics to applications, Appl. Phys. Rev. 6 (2019), https://doi.org/10.1063/1.5082215.
[3] P.K. Upputuri, M. Krisnan, M. Pramanik, Microsphere enabled subdiffraction-limited optical-resolution photoacoustic microscopy: a simulation study, J. Biomed. Opt. 22 (2016) 045001, , https://doi.org/10.1117/1.jbo.22.4.045001.
[4] Y.E. Geints, A.A. Zemlyanov, O.V. Minin, I.V. Minin, Systematic study and comparison of photonic nanojets produced by dielectric microparticles in 2D- and 3D-spatial configurations, J. Opt. (United Kingdom). 20 (2018), https://doi.org/10.1088/2040-8986/aac1d9.
[5] L.W. Chen, Y. Zhou, M.X. Wu, M.H. Hong, Remote-mode microsphere nano-imaging: new boundaries for optical microscopes, Opto-Electronic Adv. 1 (2018) 17000101–17000107, https://doi.org/10.29026/oea.2018.170001.
[6] Y.Z. Yan, L. Li, C. Feng, W. Guo, S. Lee, M.H. Hong, Microsphere-coupled scanning laser confocal nanoscope for sub-diffraction-limited imaging at 25 nm lateral resolution in the visible spectrum, ACS Nano 8 (2014) 1809–1816, https://doi.org/10.1021/nn406201q.
[7] C.M. Ruiz, J.J. Simpson, Detection of embedded ultra-subwavelength-thin dielectric features using elongated photonic nanojets, Opt. Express 18 (2010) 16805, https://doi.org/10.1364/oe.18.016805.
[8] S. cheol Kong, A. Sahakian, A. Taflove, V. Backman, Photonic nanojet-enabled optical data storage, Opt. Express 16 (2008) 13713–13719.
[9] K.J. Yi, H. Wang, Y.F. Lu, Z.Y. Yang, Enhanced Raman scattering by self-assembled silica spherical microparticles, J. Appl. Phys. 101 (2007), https://doi.org/10.1063/1.2450671.
[10] C.Y. Liu, Ultra-elongated photonic nanojets generated by a graded-index microellipsoid, Prog. Electromagn. Res. Lett. 37 (2014) 153–165, https://doi.org/10.2528/pierl12121902.
[11] A. Darafsheh, D. Bollinger, Systematic study of the characteristics of the photonic nanojets formed by dielectric microcylinders, Opt. Commun. 402 (2017) 270–275, https://doi.org/10.1016/j.optcom.2017.06.004.
[12] P.H. Wu, J. Li, K.H. Wei, W.J. Yue, Tunable and ultra-elongated photonic nanojet generated by a liquid-immersed core-shell dielectric microsphere, Appl. Phys. Express. 8 (2015), https://doi.org/10.7567/APEX.8.112001.
[13] C.Y. Liu, F.C. Lin, Geometric effect on photonic nanojet generated by dielectric microcylinders with non-cylindrical cross-sections, Opt. Commun. 380 (2016) 287–296, https://doi.org/10.1016/j.optcom.2016.06.021.
[14] Y.E. Geints, A.A. Zemlyanov, E.K. Panina, Photonic nanojet calculations in layered radially inhomogeneous micrometer-sized spherical particles, J. Opt. Soc. Am. B 28 (2011) 1825, https://doi.org/10.1364/josab.28.001825.
[15] Y.C. Shen, L.V. Wang, J.T. Shen, Ultralong photonic nanojet formed by a two-layer dielectric microsphere, Opt. Lett. 39 (2014) 4120, https://doi.org/10.1364/ol.39.004120.
[16] C.Y. Liu, Superenhanced photonic nanojet by core-shell microcylinders, Phys. Lett. Sect. A Gen. At. Solid State Phys. 376 (2012) 1856–1860, https://doi.org/10.1016/j.physleta.2012.04.035.
[17] S.C. Kong, A. Taflove, V. Backman, Quasi one-dimensional light beam generated by a graded-index microsphere: errata, Opt. Express 18 (2010) 3973, https://doi.org/10.1364/oe.18.003973.
[18] C.Y. Liu, T.P. Yen, O.V. Minin, I.V. Minin, Engineering photonic nanojet by a graded-index micro-cuboid, Phys. E Low-Dimension. Syst. Nanostruct. 98 (2018) 105–110, https://doi.org/10.1016/j.physe.2017.12.020.
[19] B. Yan, L. Yue, Z. Wang, Engineering near-field focusing of a microsphere lens with pupil masks, Opt. Commun. 370 (2016) 140–144, https://doi.org/10.1016/j.optcom.2016.03.008.
[20] J. Poco, L. Hrunesh,' 'Method of producing optical quality glass having a selected refractive index," U.S. Patent 6, 158, 244, 2008.